Cancer Chemother Pharmacol (1997) 39: 521–531

ORIGINAL ARTICLE

John L. Tonkinson · Philip Marder · Sherri L. Andis
Richard M. Schultz · Lynn S. Gossett
Chuan Shih · Laurane G. Mendelsohn

Cell cycle effects of antifolate antimetabolites: implications for cytotoxicity and cytostasis

Received: 1 April 1996 / Accepted: 5 September 1996

Abstract *Purpose*: Cell cycle-related events in CCRF-CEM lymphocytic leukemia cells were examined subsequent to inhibition of thymidylate synthase (TS) or GAR formyltransferase (GARFT) and prior to cell death or stasis. *Methods*: Cell populations were treated with the GARFT inhibitors 6*R*-5,10-dideazatetrahydrofolate (lometrexol) or LY309887, the TS inhibitor ZD1694, or the multitargeted antifolate LY231514. DNA content, nucleoside precursor incorporation and proliferating cell nuclear antigen (PCNA) expression as functions of drug treatment were assessed by multiparameter flow cytometry. Cellular respiration was measured by MTT analysis and apoptosis was detected by extraction of DNA fragments. *Results*: Cell populations treated for up to 96 h with lometrexol or LY309887 did not replicate and maintained a cell cycle distribution with distinct G_1, S and G_2/M regions. The number of S phase cells in treated populations was slightly elevated relative to control as measured by DNA content and PCNA. However, these cells were unable to incorporate 5-bromodeoxyuridine (BrdU). Throughout treatment, cells incubated with GARFT inhibitors maintained intact membranes and respired at a level comparable to untreated cells. In contrast, ZD1694 as well as LY231514, induced synchronization of the treatment population at the G_1/S interface within 12 h of drug addition. This was followed by synchronous entry of the population into S phase. After 24 h of treatment, more than 90% of the cells were capable of incorporating BrdU and stained positive for PCNA. DNA fragmentation occurred in cells treated with ZD1694 or LY231514 but not in those treated with GARFT inhibitors. In addition, the viable cells remaining after 24–48 h of treatment with ZD1694 or LY231514 were respiring at twice the level of untreated cells. *Conclusion*: These results demonstrate that the distinct endpoints of GARFT and TS inhibition are preceded by distinct cell cycle and metabolic alterations.

Key words Cell cycle · Antifolate · GARFT
Thymidylate synthase

Abbreviations *BrdU* 5-bromodeoxyuridine · *BSA* bovine serum albumin · *CV* coefficient of variation · *DACTHF* 5-deazaacyclotetrahydrofolate · *DMSO* dimethyl sulfoxide · *dNTP* deoxynucleoside triphosphate · *dTTP* deoxythymidine triphosphate · *dUTP* deoxyuridine triphosphate · *ELISA* enzyme-linked immunosorbent assay · *GARFT* glycinamide ribonucleotide formyltransferase · *LTX* lomotrexol · *LY231514* N-[4[2-(-amino-3,4-dihydro-4-oxo-7H-pyrrolo[2,3-d]pyrimidin-5-yl)ethyl]benzoyl]-L-glutamate sodium salt · *LY309887* 6*R*-2′,5′-thienyl-DDATHF · *MTA* multitargeted antifolate · *MTT* 3-[4,5-dimethylethylthiazol-2-yl]-2,5-diphenyl tetrazolium bromide · *MTX* methotrexate · *NP-40* nonidet-p40 · *NTP* nucleoside triphosphate · *OD* optical density · *PBS* phosphate-buffered saline · *PCNA* proliferating cell nuclear antigen · *PI* propidium iodide · 6*R*-*DDATHF* 6*R*-5,10-dideazatetrahydrofolate · *TE* Tris-EDTA buffer · *TS* thymidylate synthase · *ZD1694* N-[N-(3,4-dihydro-2-methyl-4-oxoquinazolin-6-ethyl)-N-methylamino]-2-thenoyl)-L-glutamic acid

J.L. Tonkinson · P. Marder · S.L. Andis · R.M. Schultz · L.S. Gossett · C. Shih · L.G. Mendelsohn (✉)
Lilly Research Laboratories, Lilly Corporate Center,
Eli Lilly and Co., Indianapolis,
IN 46285, USA
Tel. (317) 276-6924; Fax (317) 277-3652

Introduction

Inhibitors of folate-requiring enzymes which act as anticancer agents have been the subject of innumerable studies during the past four decades. Recently, several

new classes of antifolates have been developed. These include inhibitors of thymidylate synthase (TS) such as ZD1694 [14] and BW1843U89 [10], specific inhibitors of glycinamide ribonucleotide formyltransferase (GARFT) such as DACTHF (5-deazaacyclotetrahydrofolate) [3, 32], lometrexol (LTX, 6*R*-5, 10-dideaza-5,6,7,8-tetrahydrofolate, 6*R*-DDATHF) [3, 4] and LY309887 (6*R*-2′,5′-thienyldideazatetrahydrofolic acid) [13], and inhibitors of multiple enzyme targets such as LY231514 [30, 31, 35]. Comprehensive studies have reported enzyme inhibition in vitro [1, 9, 13, 31, 43], as well as intracellular biochemical alterations in response to these inhibitors, such as nucleoside and deoxynucleoside triphosphate levels (NTP and dNTP) [4, 6, 18, 26, 32, 34].

In most cell lines examined, depletion of dTTP pools by inhibition of TS results in cytotoxicity rather than cytostasis [2, 10, 33]. DNA strand breaks have been observed in cell culture after treatment with TS inhibitors. Thus, it has been postulated that TS inhibition results in apoptosis by thymineless death [15, 25, 29]. In this hypothesis, decreased pools of dTTP leads to misincorporation of deoxyuridine triphosphate (dUTP) into nascent DNA strands. Ensuing cycles of excision and repair prove futile in the absence of dTTP, and the net result is cell death [2, 6, 7]. Likewise, dihydrofolate reductase inhibitors, such as methotrexate (MTX), induce apoptosis [18]. Although MTX affects both purine and thymidylate biosynthesis, hypoxanthine, a salvage metabolite for the purine pathway, potentiates its cytotoxic activity [18, 37]. This indicates that decreased thymidylate synthesis is primarily responsible for cell death, and that low levels of purine nucleotides may be inhibitory to the apoptotic mechanism.

Treatment with antifolates which affect purine biosynthesis results in a different and distinct phenotypic endpoint. In several cells lines, treatment with LTX results in cytostasis rather than cytotoxicity [16, 23, 33]. In one study, WiDr cells treated with LTX remained morphologically intact for several days after treatment, but were unable to form colonies in soft agar [33]. In a study by Jansen et al., DACTHF caused reversible growth inhibition of WiDr spheroids and tumors, but no regression [16].

Despite detailed biochemical analysis and measurement of intracellular dNTP levels after antifolate treatment, there is little understanding of the cellular response to biochemical modulation. Inhibition of GARFT or TS results in distinct antiproliferative endpoints; these endpoints should be preceded by distinct physiological events. In this study we examined in detail cell cycle and metabolic alterations in the CCRF-CEM cell line subsequent to antifolate treatment and prior to cell death or stasis. The results demonstrate that prior to death by apoptosis, cell populations treated with the TS inhibitor ZD1694 or the multitargeted antifolate (MTA) LY231514 became synchronized at the G_1/S interface. These populations syn chronously entered S phase, maintained the ability to incorporate a nucleoside precursor into DNA and expressed proliferating cell nuclear antigen (PCNA). Prior to death by apoptosis, the respiratory levels rose to at least twice those of untreated cells. In contrast, treatment with the GARFT inhibitors LTX or LY309887 resulted in rapid cytostasis. No synchronization occurred and incorporation of nucleoside precursors decreased. Identification of these events provides insight into the role that intracellular nucleotide pool levels play in induction of cytostasis or cytotoxicity. These findings are discussed in relation to published biochemical data.

Materials and methods

Reagents and chemicals

LTX disodium salt, LY309887, LY231514 and ZD1694 were synthesized at Lilly Research Laboratories, Indianapolis, Ind. All solutions were prepared daily in phosphate-buffered saline (PBS). Propidium iodide (PI) was purchased from Molecular Probes, Eugene, Ore. RNase DNase-free, molecular weight markers and 5-bromo-2′-deoxy-uridine (BrdU) Labeling and Detection Kit I were purchased from Boehringer Mannheim Biochemicals, Indianapolis, Ind. MTX, MTT, NP-40 and phenol/chloroform/isoamyl alcohol were purchased from Sigma Chemical Company, St. Louis, Mo.

Cell culture

CCRF-CEM cells (obtained as a gift from St. Jude's Children Research Hospital, Memphis, Tenn.) were grown at 37 °C in a humid atmosphere containing 5% CO_2 in RPMI-1640 medium (Whittaker Bioproducts, Walkersville, Md.) supplemented with 10% dialyzed fetal bovine serum (Gibco BRL, Grand Island, N.Y.). The culture was maintained in log-phase growth. For all experiments, cells were seeded in fresh medium at a density of 2×10^5 cells/ml, and allowed to incubate overnight prior to treatment. All cell counts were made with a hematocytometer using trypan blue exclusion to distinguish between live and dead cells.

Analysis of DNA content

Working strength solution of Vindelov's PI stain [27] was made with 5 m*M* Tris buffer, pH 7.4, 5 m*M* NaCl, 0.05% NP-40 and 0.04 mg/ml PI. Immediately prior to use, RNase DNase-free was added (0.15 units/ml).

Following the indicated treatment, aliquots of cells were removed from culture and separated from medium by low-speed centrifugation. The pellet was suspended in 300 µl PBS and the cells were fixed by addition of 700 µl reagent grade methanol drop-wise while vortexing gently. The cells were stored at 4 °C for at least 1 h. Fixed cells were pelleted at 2000 *g*, 10 min, and resuspended in 500 µl Vindelov's PI stain. The PI fluorescence was determined by flow cytometry.

Analysis of BrdU incorporation

BrdU incorporation was detected using the BrdU Labeling and Detection Kit I. The procedure was modified from Vanderplasschen

et al. [41]. Cells were exposed to compounds at the concentrations and for the periods indicated. After treatment, aliquots of cells were incubated with 10 μ*M* BrdU at 37 °C for 1 h. The cells were collected by centrifugation (300 *g*, 5 min, 4 °C) and resuspended in 200 μl PBS. Cells were fixed by the addition of 1 ml 70% ethanol in 50 m*M* glycine buffer, pH 2.0, and were stored at 4 °C for at least 2 h. Fixed cells were pelleted by centrifugation at 2000 *g* (10 min, 4 °C), and washed once with PBS containing 2.5% bovine serum albumin (PBS/BSA). Cell pellets were resuspended in 300 μl of the anti-BrdU working solution supplied in the BrdU Labeling and Detection Kit I, and incubated at 37 °C for 1 h. Cells, pelleted as described above and washed once with PBS/BSA, were resuspended by gentle vortexing in 200 μl antimouse-Ig-fluorescein working solution supplied in the kit and incubated at 37 °C for 1 h. PBS/BSA (500 μl) was added to each sample, and the supernatant was removed after centrifugation. Cell pellets were resuspended in 300 μl Vindelov's PI stain and analyzed by two-parameter flow cytometry.

Flow cytometry and data analysis

Flow cytometric analysis was performed on a Coulter Electronics (Hialeah, Fl.) XL analytical cytometer. Excitation of both PI and fluorescein was accomplished with the 488-nm line of an argon laser (15 mW). The emission intensities of the fluorescein signal were collected using a linear amplifier and plotted on a log scale, and the emission intensities of the PI signal were collected using a linear amplifier and plotted on a linear scale. For each experimental condition, list mode data from 1×10^4 cells was analyzed.

Single color PI data were integrated with MultiCycle AV software (Phoenix Flow Systems, San Diego, Calif.). The G_1 and G_2/M regions of each histogram were fitted to Gaussian functions, and the S phase region was fitted to an *n*th order polynomial.The order of the S phase polynomial was chosen to best reflect the observed profile of a given histogram. Two color data were analyzed using WinList software (Verity Software House, Topsham, Me.). The limit of detection of incorporated BrdU was determined by nonspecific binding of the mouse-Ig-fluorescein antibody in the absence of primary antibody.

Detection of nuclear PCNA

Nuclear PCNA was detected flow cytometrically by the method of Lohr et al. [20]. At each time-point, approximately 1×10^6 cells were harvested from each treatment, and suspended in 0.5 ml PBS/BSA, 0.2% EDTA and 0.25% Triton X 100, and placed on ice for 15 min. The cells were then harvested by centrifugation (2000 *g*, 5 min), resuspended in 50 μl PBS and placed in 3 ml methanol. The samples were stored at −20 °C for at least 2 h. Additional permeabilization was accomplished by suspending the cells in 0.5 ml PBS/BSA with 0.5% Triton X 100 for 15 min at room temperature. The samples were washed with PBS/BSA and taken up in a 23G syringe several times to break up aggregates, after which the buffer was removed by centrifugation. FITC-conjugated mouse antihuman PCNA antibody (PharMingen, San Diego, Calif.) was added to each sample, diluted 1:10 in PBS/BSA, 30 min, room temperature. PBS/BSA (1 ml) was added and the samples centrifuged and washed twice with PBS/BSA. Aggregates were again broken up with a 23 G syringe. The samples were suspended in 0.5 ml Vindelov's PI stain and analyzed by dual-parameter flow cytometry as described above.

DNA fragmentation assay

Soluble DNA was isolated following the method of Lindenboim et al. [19]. Briefly, 2.5×10^6 cells were isolated and lysed in 5 m*M* Tris, pH 7.4, 20 m*M* EDTA and 0.5% Triton X 100 (4 °C, 20 min). The samples were centrifuged at 27 000 *g*, 4 °C for 15 min, and the supernatant was extracted twice with phenol/chloroform/isoamyl alcohol and once with chloroform. The aqueous layer was precipitated with 0.13 *M* NaCl (final) and three volumes of 100% ethanol. The pellet was dissolved in 100 μl Tris-EDTA buffer, pH 7.4 (TE), with RNase DNase-free (0.15 units/ml) and incubated at 37 °C overnight. Ethanol precipitation was repeated and the pellet dissolved in 10 μl TE buffer (37 °C, 30 min). DNA concentration and purity were determined spectrophotometrically; 2.5 μg from each sample was electrophoresed in 1× Tris-acetate-EDTA buffer (Gibco BRL, Grand Island, N.Y.) on a 1.2% agarose gel containing 0.5 μg/ml ethidium bromide. DNA bands were visualized by UV illumination.

MTT and cell viability studies

CEM cells were seeded at 2×10^5/ml in complete medium in 96-well plates (100 μl/well), and incubated at 37 °C for 16–24 h. Drug or control medium were added at the indicated concentrations, and measurements taken at the indicated times. At each time-point, duplicate determinations of cell density and viability (trypan blue exclusion) were determined. MTT 10 μl was added to three wells from each treatment group, and the plate was incubated at 37 °C for 40 min. DMSO (100 μl) was then added to each well with gentle stirring. The OD_{540} of each well was measured in an ELISA plate reader.

Results

Alterations in cell cycle profiles in response to antifolates

The DNA content of CCRF-CEM cells subsequent to antifolate treatment was examined to study the cellular response to GARFT or TS inhibition prior to cytostasis or cytotoxicity. Cultures were allowed to enter log-phase growth prior to dosing to distinguish between effects on cell proliferation and effects on reentry into the cell cycle. Cells were seeded at 2×10^5/ml approximately 16 h prior to compound addition. Each drug treatment group was maintained as a single culture and $1–2 \times 10^6$ cells were removed for fixation and analysis at the indicated times. Under these conditions, untreated populations underwent 1.5–1.8 doublings in a 24-h period. In these experiments, the final concentrations of the antifolates were: LTX, 129 n*M*; LY309887, 29 n*M*; LY231514, 210 n*M*; and ZD1694, 22 n*M*. The concentrations were equipotent based on cellular respiration assays to assess inhibitory potency at 72 h after compound addition (data not shown). These concentrations prevented population doubling and no toxicity was observed during the first 24 h of exposure.

Representative DNA content histograms are shown in Fig. 1. In untreated control cells, there was little change in the DNA content over time and the cell cycle profiles remained fairly consistent throughout the time course. The GARFT inhibitors LY309887 (29 n*M*; Fig. 1) and LTX (129 n*M*; data not shown) induced a modest increase in the number of cells containing S phase DNA beginning 6 h after dosing. At $t = 24$ h, the

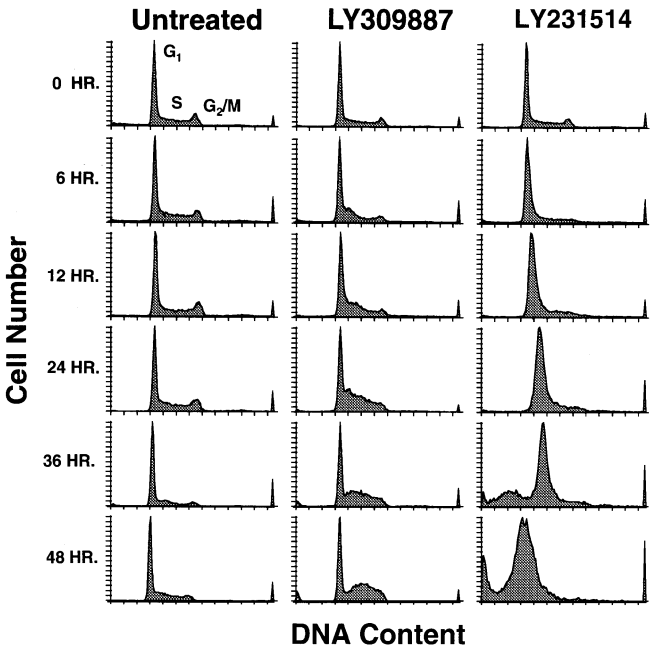

Fig. 1 Histograms of time-dependent alterations in DNA content of antifolate-treated CEM cells. Log-phase CEM cells were incubated with LY309887 (29 n*M*) or LY231514 (210 n*M*) at 37 °C. At the indicated times after dosing, cells were fixed with methanol and stained with PI as described in Materials and methods. The linear fluorescence intensity of each cell was determined on a Coulter XL flow cytometer. Regions corresponding to G_1, S and G_2/M DNA content are shown on the untreated $t = 0$ h histogram

area of the S phase region appeared to be substantially greater than at $t = 0$. A similar profile was observed at 48 h post-dose (Fig. 1) and was maintained up to 96 h in culture (data not shown). There was no doubling of the populations treated with LY309887 (29 n*M*) or LTX (129 n*M*) for up to 96 h (data not shown). This is consistent with the loss of cell proliferation following treatment with GARFT inhibitors that has previously been described [3, 32, 33]. Thus, the increased number of cells containing S phase DNA within the population is indicative of either a slowed rate of progression through S phase, or a block at the S/G_2 transition. Both of these possibilities may contribute to the observed profile. A distinct G_1 peak was observed at all times during treatment. Furthermore, the G_1 peak coefficient of variation (CV) was consistently less than 4%, suggesting a normal distribution of cells in the G_1 or G_0 phase of the cell cycle. It is also possible that GARFT inhibition forced cells into G_0, although this analysis does not distinguish between G_1 and G_0. Increasing the concentration of LY309887 or LTX tenfold (290 n*M* and 1.29 μ*M*, respectively) resulted in cell cycle profiles identical to those with the lower concentrations, with no evidence of cytotoxicity. Tenfold lower concentrations (2.9 n*M* and 12.9 n*M*, respectively) had no effect on the cell cycle prolfiles or the growth rates of CEM cells.

These results are in sharp contrast to the DNA content profiles observed for cells treated with the TS inhibitor ZD1694, or the MTA LY231514 (210 n*M*; Fig. 1). The disappearance of a discernible G_2/M peak at 6 h, followed by a broadening of the G_1 peak at 12 h is indicative of a synchronization of the population in the G_1 phase. The CV of the G_1 peak, which was normally less than 4%, increased to over 10% at 12 h, suggesting an increase in the number of cells containing diploid DNA. It is interesting to note that synchronization occurred prior to a complete doubling of the population. There are indications that antifolates, including inhibitors of TS, are S-phase specific [15]. However, the results suggest that the initial event was a transient block at the G_1/S transition followed by a delayed progression of G_1 cells into S phase. In contrast, cells in S and G_2/M completed their cycle. After 12–24 h, the primary cell population peak shifted to higher intensity, demonstrating a synchronous entry into S phase. Thus, ZD1694 and LY231514 had similar cell cycle effects while GARFT inhibitors had distinct mechanisms of cell cycle inhibition.

After 36 h of treatment with ZD1694 or LY231514, a sub-G_1 peak developed (Fig. 1). Profiles of this type result from the presence of apoptotic cells [8]. When apoptotic cells are fixed with alcohol for DNA analysis, small DNA fragments are washed out from the cells leaving intact cells with a reduced DNA content and thus reduced PI intercalation. At 48 h after treatment, the apoptotic peak accounted for nearly 100% of the cells. The appearance of apoptotic cells in response to treatment with ZD1694 or LY231514 occurred in the first passage through the cycle after synchronization. The apoptotic peak was absent in the control, and LTX- and LY309887-treated populations.

Integration of histograms was accomplished by modeling the data with MultiCycle AV software as described in Materials and methods. The percentage of cells from each treatment group which contained G_1 and S phase DNA is shown in Fig. 2. The percentage of viable cells containing G_2/M DNA accounted for less than 10% of the total at all times, therefore the data have not been included on the graphs. Within 12 h of exposure, LTX and LY309887 induced a modest increase in the number of S phase cells and a decrease in the number of G_1 cells relative to the untreated population (Fig. 2 A, B, C). There was a similar increase in the number of cells expressing the S phase-specific PCNA (data not shown). PCNA levels were measured by dual-parameter flow cytometry in order to confirm the S phase buildup. Approximately 75% of the treated populations expressed nuclear PCNA after 48 h of treatment with LTX or LY309887. This parallels the increased number of cells containing S phase DNA.

A marked increase in size of the G_1 population was observed after 8–10 h of treatment with the TS inhibitor ZD1694 and with the MTA LY231514 (Fig. 2 D, E).

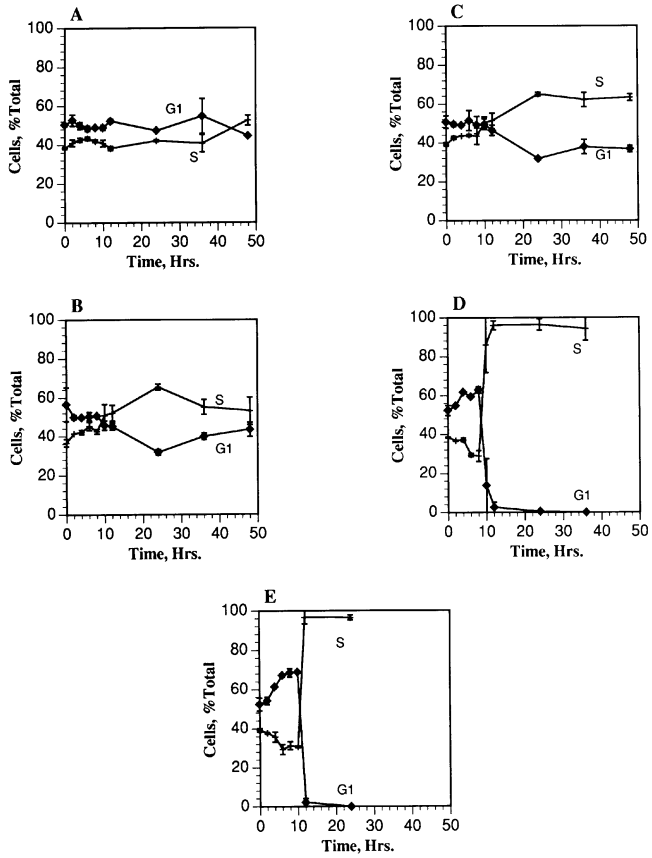

Fig. 2A–E Percentage of total cells in each treatment population containing G_1 and S phase DNA. DNA histograms were integrated as described in Materials and methods. The percentage of cells containing G_1 or S phase DNA is plotted as a function of treatment duration. Treatments are: **A** untreated population; **B** LTX (129 n*M*); **C** LY309887 (29 n*M*); **D** LY231514 (210 n*M*); **E** ZD1694 (22 n*M*). *Error bars* represent the range of values obtained from duplicate experiments

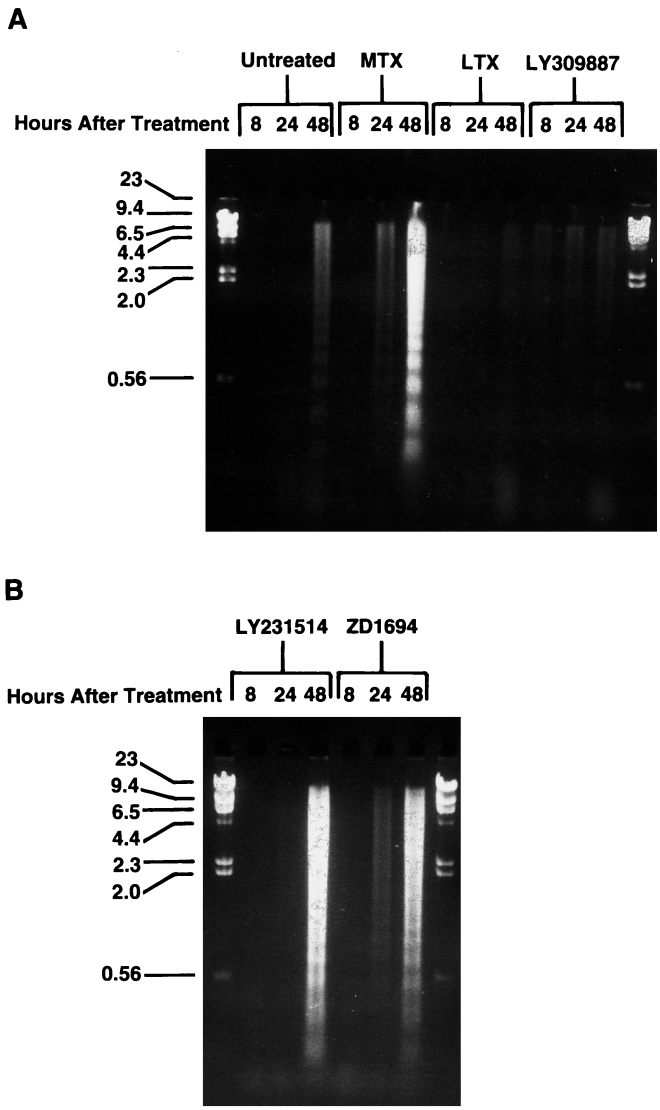

Fig. 3A, B Selective induction of DNA fragmentation by inhibitors of TS or DHFR. CEM cells were incubated with: **A** MTX (66 n*M*), LTX (129 n*M*) or LY309887 (29 n*M*); or **B** LY231514 (210 n*M*) or ZD1694 (22 n*M*) at 37 °C. Soluble DNA (27 000 *g*) was isolated from 2.5×10^6 cells in each treatment population after 8, 24 and 48 h of incubation as described in Materials and methods. DNA (2.5 µg) from each sample was electrophoresed on a 1.2% agarose gel containing 0.5 mg/ml ethidium bromide (1× TAE, 125 V, 3 h). DNA bands were visualized by UV illumination

This was followed by a complete disappearance of the G_1 population, and an increase in number of S phase cells to more than 90% of the total population. Cells with measurable DNA content were no longer observed after 36 h of treatment with either LY231514 or ZD1694 (Fig. 2D, E). Nuclear PCNA was expressed in more than 90% of the cells in the treated populations confirming that these populations were in S phase (data not shown). This analysis confirms that at these concentrations, ZD1694 and LY231514 caused synchronization of CCRF-CEM cells in G_1 approximately 8–10 h after treatment; this event was followed by a uniform entry of all cells in the population into S phase.

Selective induction of DNA fragmentation

The sub-G_1 peaks observed in the DNA histograms for ZD1694 and LY231514 were interpreted to be apoptotic cells. To confirm this possibility, soluble DNA (27 000 *g*) was isolated from treated and untreated control populations at 8, 24 and 48 h after dosing, and separated by agarose gel electrophoresis (Fig. 3). In the untreated population, some fragmentation was observed at the 48-h point (72 h after plating). This is not unexpected for an aging population of lymphocytes. Furthermore, the cell density had decreased between 24 and 48 h indicating that some cell death had occurred. Significantly more fragmentation, relative to control, was apparent in the cells treated with LY231514 and

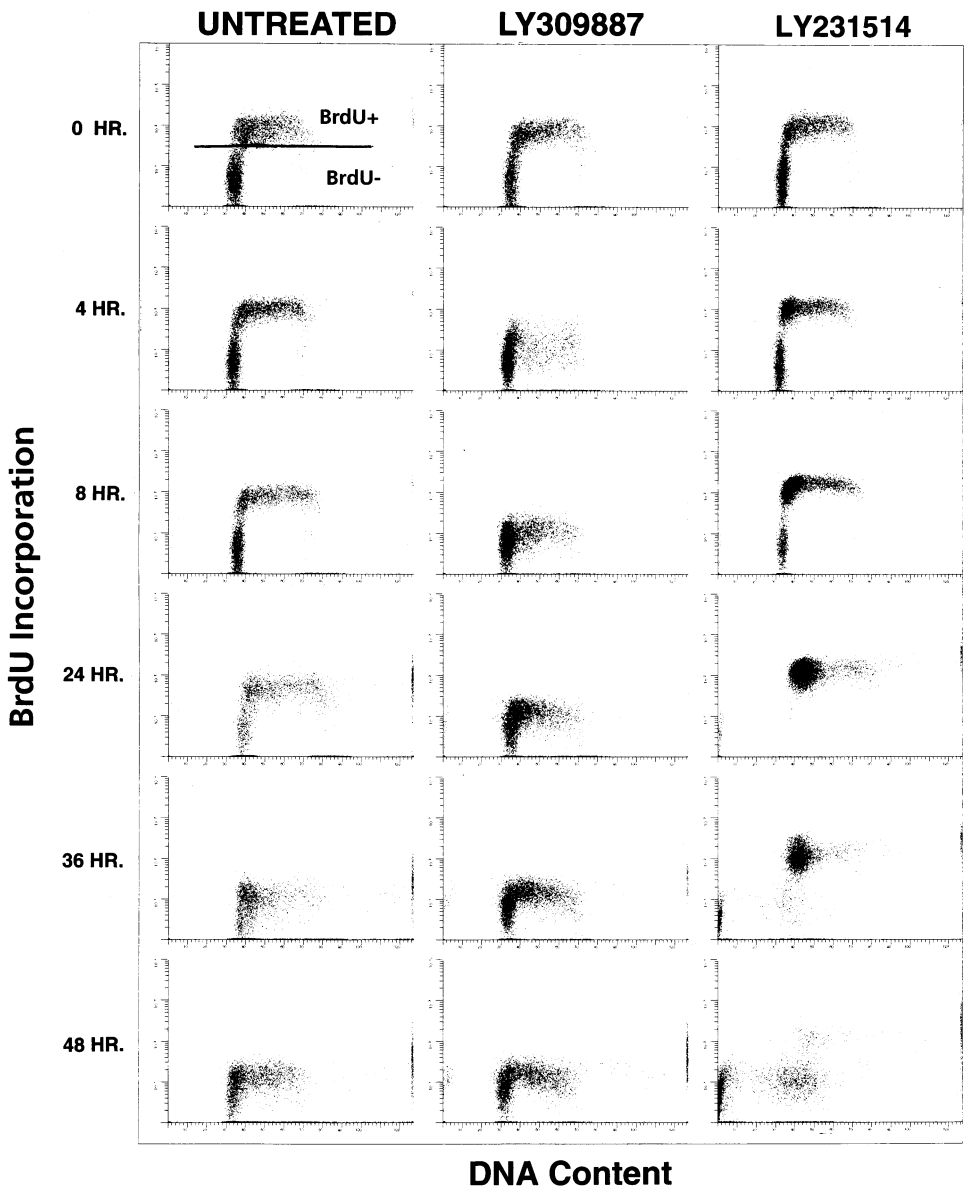

Fig. 4 Time-dependent alterations in BrdU incorporation of antifolate-treated CEM cells. CEM cells were treated with LY309887 (29 n*M*) or LY231514 (210 n*M*) for the indicated times at 37 °C. Following treatment, the cells were incubated at 37 °C for 1 h with BrdU (10 μ*M*), after which they were fixed in ethanol/glycine (pH 2.0). BrdU incorporation was visualized by immunofluorescence and the DNA content was measured by PI fluorescence as described in Materials and methods. The limit of detection of BrdU was determined by the nonspecific binding of the secondary fluorescent antibody in the absence of the primary antibody. This limit is shown in the untreated $t = 0$ h plot

ZD1694 at both 24 and 48 h. MTX was included as a positive control. Resolution of the lower molecular weight bands revealed the presence of distinct 180–200 bp fragments. In contrast, no DNA degradation was observed at any time in the populations treated with the GARFT inhibitors LTX and LY309887.

Precursor incorporation in antifolate-treated cells

Increased numbers of cells containing S phase DNA were observed in populations treated with all inhibitor classes. However, GARFT inhibition resulted in cytostasis, whereas ZD1694 and MTA caused cytotoxicity by apoptosis. In order to examine the difference in S phase accumulation by GARFT inhibition versus TS inhibition, the ability of CCRF-CEM cells to incorporate BrdU into newly synthesized DNA was examined. Incorporation of BrdU into DNA demonstrates that the cell has the potential to synthesize DNA. This includes activation of the precursors to nucleoside triphosphates, and incorporation of activated nucleoside. We used dual-parameter flow cytometry to correlate DNA content (PI fluorescence) with incorporation of BrdU [12]. In the following experiments, at the end of each treatment period, $1–2 \times 10^6$ cells were incubated for 1 h with BrdU as described in Materials and methods. Thus, only cells which were actively synthesizing DNA at the end of treatment would stain positive for BrdU.

Figure 4 illustrates data from a representative experiment of the effects of LY309887 and LY231514 on the

Table 1 CCRF-CEM cell growth, respiration and membrane integrity in response to antifolate treatment. CCRF-CEM cells were plated at $t = 0$ h. The indicated compounds were added at 24 h and incubation continued for an additional 48 h. The number of cells in each treatment population was determined with a hematocytometer. Respiratory ability was determined by MTT reduction as described in Materials and methods. Respiratory capacity was calculated on a per cell basis as determined from the number of trypan blue excluding cells and normalized relative to the respiratory capacity of control cells. All values shown are the average of three independent experiments ± SEM

Treatment	MTT signal (OD_{540})	Change in cell number (%)	Respiratory capacity (OD_{540}/viable cell) (% untreated)	Trypan blue positive (% total)
Untreated	0.481 ± 0.043	+ 304 ± 33	100	1.0 ± 0.261
LTX (129 n*M*)	0.255 ± 0.02	+ 91 ± 3	130 ± 3	1.3 ± 0.7
LY309887 (29 n*M*)	0.156 ± 0.016	+ 40 ± 14	100 ± 14	3.8 ± 0.6
LY231514 (210 n*M*)	0.215 ± 0.016	−1.5 ± 11	230 ± 15	31 ± 3.2
ZD1694 (22 n*M*)	0.156 ± 0.021	− 31 ± 12	240 ± 57	50 ± 5.8

ability of CCRF-CEM cells to incorporate BrdU. In untreated control cells, a gradual decrease in the number of BrdU-positive cells was observed over 48 h. The decrease occurred uniformly from the G_1 and S regions, indicating an overall decline in BrdU incorporation in these cells. This is not unexpected for a population entering the lag phase. A similar but more rapid loss was observed for cells treated with LY309887. After 24 h of treatment, less than 10% of the population incorporated BrdU. The loss of BrdU-positive cells may be due to either a lack of precursor activation caused by decreased ATP levels, or a decreased rate of DNA synthesis. These two possibilities are not mutually exclusive. LTX-treated cells responded in a similar manner (data not shown). Although an increase in the number of cells containing S phase DNA was observed following GARFT inhibition (Figs. 1, 2), we were not able to detect a corresponding increase in the number of cells which incorporated BrdU. To account for the elevated number of S phase cells, limited DNA synthesis must have occurred, but the rate was below our limit of detection.

A distinctly different profile was obtained for cells treated with LY231514 (Fig. 4) and ZD1694 (data not shown). In response to treatment, a marked increase was observed in the number of BrdU-positive cells containing G_1 DNA. This region has been defined as the G_1/S interface [39]. These data indicate that the G_1 DNA content peak was composed of two populations of cells, BrdU-positive and BrdU-negative. The number of BrdU-positive cells within this peak increased with duration of treatment. After 24–36 h of treatment, more than 80% of the population incorporated BrdU, implying that the cells had the capacity to synthesize DNA. The heterogeneous distribution observed at 48 h is indicative of cell death.

Respiration and cell viability

The respiratory ability of each population in relation to the rate of growth was examined. Inability of a cell population to reduce MTT is often used as a criterion to define cytotoxicity [24]. However, loss of MTT reduction in a treatment population is not necessarily a consequence of cell death; if the treatment population were growing at a slower rate than the control population, a lower signal would result.

The ability of CEM cells to reduce MTT was determined after 48 h of antifolate treatment (Table 1). For all treatments, the absolute signal was less than or equal to one-half that of the untreated control population. However, as shown in Table 1, cell growth continued in the presence of GARFT inhibitors, albeit at a slower rate than in control cells. In contrast, in the presence of ZD1694 or LY231514, the cell number declined over 48 h. When the MTT signal was normalized for viable (trypan blue excluding) cells it became apparent that after 48 h of continuous treatment, cells treated with GARFT inhibitors were respiring at the same level as untreated cells, but cells treated with TS inhibitor were respiring at approximately twice that level. It is also possible that reduction of tetrazolium salts by trypan blue-positive cells was occurring. However, even if this were the case, the signal-to-cell ratio was still greater than for the control population.

In untreated and GARFT inhibitor-treated populations, the cell number as well as the MTT signal increased with time (Fig. 5). However, the rate of increase in MTT signal was less than the rate of cell proliferation. In contrast, the change in the MTT signal for ZD1694- or LY231514-treated cells closely paralleled the change in cell number. Thus, the respiratory signal-to-cell ratio was virtually identical for control and GARFT inhibitor-treated cells, but was substantially higher for the TS inhibitor- and MTA-treated cells (Table 1).

The viability of cells in each treatment group was assessed by their ability to exclude trypan blue (Table 1). More than 95% of the untreated and GARFT inhibitor-treated cells excluded trypan blue after 48 h of continuous treatment. However, 30–50% of TS inhibitor- and MTA-treated cells stained positive for trypan blue. These results indicate that although

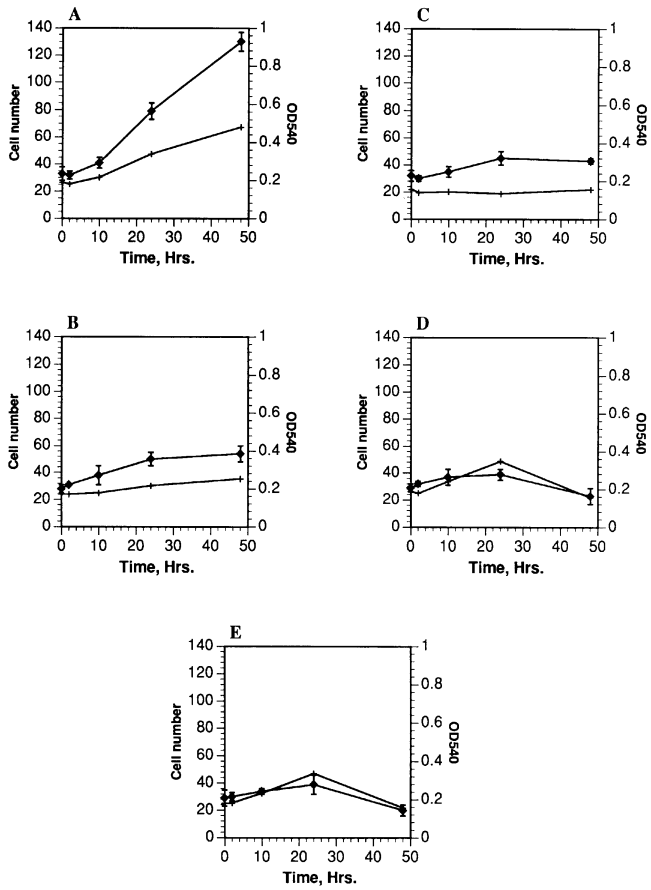

Fig. 5A–E Cell proliferation and respiration in response to antifolate treatment. At the indicated times during treatment, the number of viable cells per well ($\times 10^{-3}$) (◆) was determined by trypan blue exclusion, and the ability of each population to reduce MTT (+) was measured as described in Materials and methods. The treatments are: **A** untreated population; **B** LTX (129 n*M*); **C** LY309887 (29 n*M*); **D** LY231514 (210 n*M*); **E** ZD1694 (22 n*M*). Each point is the average of triplicate measurements and error bars represent the standard error (SEM)

GARFT inhibition slowed the rate of cell growth, normal respiration continued. Furthermore, membrane breakdown, a traditional hallmark of death, did not occur.

Discussion

Antifolate antimetabolites induce either antiproliferative or cytotoxic responses depending on which biosynthetic pathways are affected. In general, inhibitors of thymidylate synthesis induce cytotoxicity through apoptosis, whereas inhibitors of purine synthesis cause cytostasis. For example, Pizzorno et al. [26] have demonstrated growth inhibition but not apoptosis in CEM lymphoma cells treated with the GARFT inhibitor LTX. Interestingly, although LTX treatment results in decreased pools of both ATP and GTP, differential repletion of both nucleotides demonstrates that GTP depletion is primarily responsible for the observed effects. A similar study by Jansen et al. [16] has confirmed that LTX as well as DACTHF treatment of WiDR spheroids in vitro and tumors in vivo results in growth inhibition but not regression. Smith et al. [33] have reported that WiDR cells treated with LTX are unable to form colonies in soft agar. Thus, the authors concluded that LTX is indeed cytotoxic. However, the initial treatment with LTX did not cause the morphological changes induced by ZD1694, and a substantial number of cells remained adherent to the culture plates. In addition, DDATHF induces maturation and differentiation of HL60 promyelocytic leukemia cells [34]. This phenomenon is attributed to a decrease in GTP levels and not to decreased ATP levels. In contrast, DNA fragmentation, decreased cell numbers and apoptosis have been reported for populations treated with several different TS inhibitors including ZD1694, CB3717 and AG331 [21, 25, 29]. Potentiation of the cytotoxicity of TS inhibitors by the addition of exogenous purines indicates that the cytotoxic mechanism is dependent on a balance between purine and pyrimidine pools [6].

Our results agree with previously published reports describing the distinct phenotypic endpoints of GARFT and TS inhibition [33]. LY309887, the thioenyl analogue of LTX, mimics LTX in causing cytostasis of CEM populations. At the concentrations studied, we observed no doubling or regression of the population during 96 h of continuous exposure. Conversely, the TS inhibitor ZD1694 as well as the multitargeted compound LY231514 prevented growth during the first 24 h of exposure, then caused cell death via apoptosis.

Alterations of the cell cycle in response to antifolate treatment have been recognized for many years [28, 38, 39]. Originally, it was thought that decreased intracellular dNTP levels result in slowed progression through S phase followed by cell death [5, 39]. Other studies suggest that prior to cell death, MTX synchronizes cells either in G_1 or at the G_1/S boundary [5, 28, 36, 39, 40]. Human bone marrow cells treated with MTX for 24 h accumulate in early G_1 [17]. Despite these observations, the relationship between population synchrony and cell death has not been explained.

Our observations indicate that antifolate-induced apoptosis was preceded by a transient block at the G_1/S interface and synchronous entry into S phase. It is not clear why synchronization occurs in response to treatment with these compounds. Although TS inhibitors are considered S phase-specific drugs [15], it appears that TS inhibition also affects cells in other phases of the cell cycle. Interestingly, nontoxic concentrations of LY231514 also synchronized the population within 24 h. However, after an additional 24 h in the

presence of the drug, the population had doubled and was again asynchronous (data not shown).

It is possible that the increase in the number of cells containing G_1 DNA after 8–10 h of treatment with LY231514 or ZD1694 (Figs. 1, 2) was caused by entry of cells into the quiescent G_0 phase of the cell cycle. However, the detection of BrdU incorporation demonstrates that the G_1 peak comprised two subpopulations: a population able to incorporate BrdU, and a population unable to incorporate BrdU. The former probably represents cells at the G_1/S interface. Subsequently, a synchronous increase in DNA content was observed as well as an increase in the number of cells expressing PCNA, indicating entry into S phase. It can be inferred from these results that ZD1694 and LY231514 do not inhibit initiation of DNA synthesis, and that initiation of DNA synthesis is necessary for cell death to occur.

LTX and LY309887 produced minor alterations in the cell cycle profiles of CEM cells. There was an increase in the number of cells containing S phase DNA, as well as the number of cells expressing PCNA, but population synchrony was not evident. Cells in the S phase region of these histograms were unable to incorporate BrdU, within our limits of detection. The apparent lack of BrdU incorporation may be the consequence of decreased pools of ATP and GTP so that precursor phosphorylation did not occur. This hypothesis provides an explanation for the lack of population doubling in response to GARFT inhibtion. Cells in S phase at the time of drug treatment were unable to complete duplication of their genome and enter mitosis.

Our results confirm and extend previous reports concerning the effects of LTX and ZD1694 on the cell cycle [4, 11]. A buildup of cells with S phase DNA content in the murine L1210 cell line (1 μM, 48 h) and the human ovarian carcinoma cell line SW626 (0.5 μM, 24 h) has been reported following LTX treatment [4, 11]. Erba et al. [11] observed decreased BrdU incorporation in SW626 cells following LTX treatment. However, in these studies, no correlation relating these observations to cytotoxicity was examined. Treatment of human colon carcinoma cells with ZD1694 delays progression through S phase [22]. However, to the best of our knowledge, there are no reports relating this delay to alterations in DNA synthetic activity prior to apoptosis.

The comparison presented here of cell cycle alterations in response to treatment of CEM cells with LTX, LY309887, ZD1694 and LY231514 provides a bridge between biochemical modulation and cytostasis or cytotoxicity. Several groups have proposed that a critical balance of nucleotide pools determines the fate of a cell. Chong and Tattersall measured dATP and dTTP pools in L1210 cells after treatment with either LTX or the TS inhibitors ZD1694, CB3717 or FdUrd [6]. LTX reduced both dATP and dTTP levels to approximately 30% of control, whereas treatment with the TS inhibitors reduced dTTP levels, but increased dATP levels to two to three times that of control. Combinations of DDATHF with the TS inhibitors were less toxic than the TS inhibitors alone, and reduced both nucleotide levels. Our results suggest that GARFT inhibition results in an inability of the cell to activate nucleosides and traverse S phase. These functions appear to be necessary for apoptosis induced by inhibitors of TS. This is in agreement with the thymineless death mechanism which has been proposed [15, 25, 29].

Another possible explanation for the lack of apoptosis after GARFT inhibition is found in our observation that respiration increases in cells which are beginning to undergo apoptosis. A similar observation has been reported for human leukemia cells in which apoptosis is induced by the anti-BAL monoclonal antibody [42]. Cytotoxicity is often measured by the inability of a population to reduce MTT through aerobic respiration [24]. However, as Table 1 and Fig. 5 demonstrate, decreased aerobic activity does not necessarily coincide with cell death. Cells treated for 48 h with LY231514 or ZD1694 respired at twice the level of untreated cells, but almost 50% of the population was nonviable as determined by trypan blue exclusion. In the presence of LTX and LY309887 cell proliferation ceased, but the cells were respiring at the same level as untreated control cells. Thus, it is possible that GARFT inhibition precludes apoptosis by eliminating the energy source needed for increased respiration and DNA synthesis, whereas increased ATP levels after TS inhibition actually facilitate apoptosis.

The results presented in this study identify key cellular responses to biochemical modulation by antifolates. We have observed cell cycle alterations which provide insight into the physiological effects of decreased nucleotide pools. The different endpoints, cytostasis or cytotoxicity, of GARFT inhibition vs TS inhibition can be related to the cellular responses to decreased dATP or dTTP. In addition, the effects of the multitargeted antifolate, LY231514, are virtually identical to those of a pure TS inhibitor in the CEM cell line.

Acknowledgement We gratefully acknowledge Larry Mann for technical assistance on the flow cytometer.

References

1. Baldwin SW, Tse A, Gossett LS, Taylor EC, Rosowsky A, Shih C, Moran RG (1991) Structural features of 5,10-dideaza-5,6,7,8-tetrahydrofolate that determine inhibition of mammalian glycinamide ribonucleotide formyltransferase. Biochemistry 30:1997–2006
2. Banks SD, Waters KA, Barrett LL, Dickerson S, Pendergast W, Smith GK (1994) Destruction of WiDr multicellular tumor spheroids with the novel thymidylate synthase inhibitor 1843U89 at physiological thymidine concentrations. Cancer Chemother Pharmacol 33:455–459

3. Beardsley GP, Taylor EC, Grindey GB, Moran RG (1986) Deaza derivatives of tetrahydrofolic acid. A new class of folate antimetabolite. In: Cooper BA, Whitehead VM (eds) Chemistry and biology of pteridines. Walter de Gruyter, Berlin, pp 953–957
4. Beardsley GP, Moroson BA, Taylor EC, Moran RG (1989) A new antimetabolite, 5,10-dideaza-5,6,7,8-tetrahydrofolate is a potent inhibitor of de novo purine synthesis. J Biol Chem 264 : 328–333
5. Bruce-Gregorios JH, Soucy D, Chen MG, Benson N (1991) Effect of methotrexate on cell cycle and DNA synthesis of astrocytes in primary culture: flow cytometric studies. J Neuropathol Exp Neurol 50 : 62–72
6. Chong L, Tattersall MHN (1995) 5,10-dideazatetrahydrofolic acid reduces toxicity and deoxyadenosine triphosphate pool expansion in cultured L1210 cells treated with inhibitors of thymidylate synthase. Biochem Pharmacol 49 : 819–827
7. Curtin NJ, Harris AL, Aherne GW (1991) Mechanism of cell death following thymidylate synthase inhibition: 2′-deoxyuridine-5′-triphosphate accumulation, DNA damage, and growth inhibition following exposure to CB3717 and dipyridamole. Cancer Res 51 : 2346–2352
8. Darzynkiewicz Z, Bruno S, Del Bino G, Gorczyca W, Hotz MA, Lassota P Traganos F (1992) Features of apoptotic cells measured by flow cytometry. Cytometry 13 : 795–808
9. Dev IK, Dallas WS, Ferone R, Hanlon M, McKee DD, Yates BB (1994) Mode of binding of folate analogs to thymidylate synthase. J Biol Chem 269 : 1873–1882
10. Duch DS, Banks S, Dev IK, Dickerson SH, Ferone R, Heath LS, Humphreys J, Knick V, Pendergast W, Singer S, Smith GK, Waters K, Wilson HR (1993) Biochemical and cellular pharmacology of 1843U89, a novel benzoquinoline inhibitor of thymidylate synthase. Cancer Res 53 : 810–818
11. Erba E, Sen S, Sessa C, Vikhanskaya FL, Incalci MD (1994) Mechanism of cytotoxicity of 5,10-dideazatetrahydrofolic acid in human ovarian carcinoma cells in vitro and modulation of the drug activity by folic or folinic acid. Br J Cancer 69 : 205–211
12. Gray JW, Dolbeare F, Pallavicini MG (1990) Quantitative cell-cycle analysis. In: Melamed, MR, Lindmo T, Mendelsohn ML (eds) Flow cytometry and sorting, 2nd edn. Wiley, New York, Chichester Brisbane Toronto Singapore, pp 445–467
13. Habeck LL, Leitner TA, Shackelford KA, Gossett LS, Schultz RM, Andis SL, Shih C, Grindey GB, Mendelsohn LG (1994) A novel class of monoglutamated antifolates exhibits tight-binding inhibition of human glycinamide ribonucleotide formyltransferase and potent activity against solid tumors. Cancer Res 54 : 1021–1026
14. Jackman AL, Taylor GA, Gibson W, Kimbell R, Brown M, Calvert AH, Judson IR, Hughes LR (1991) ICI D1694, a quinazoline antifolate thymidylate synthase inhibitor that is a potent inhibitor of L1210 tumor cell growth in vitro and in vivo: a new agent for clinical study. Cancer Res 51 : 5579–5586
15. Jackson RC (1984) Biological effects of folic acid antagonists with antineoplastic activity. Pharmacol Ther 25 : 61–82
16. Jansen M, Dykstra M, Lee JI, Stables J, Topley P, Knick VC, Mullin RJ, Duch DS, Smith GK (1994) Effects of purine synthesis inhibition on WiDr spheroids in vitro or on WiDr or colon 38 tumors in vivo. Biochem Pharmacol 47 : 1067–1078
17. Krishan A, Pitman SW, Tattersall MHN, Paika KD, Smith DC, Frei E (1976) Flow microfluorometric patterns of human bone marrow and tumor cells in response to cancer chemotherapy. Cancer Res 36 : 3813–3820
18. Kwok JBJ, Tattersall MHN (1992) DNA fragmentation, dATP pool elevation and potentiation of antifolate cytotoxicity in L1210 cells by hypoxanthine. Br J Cancer 65 : 503–508
19. Lindenboim L, Diamond R, Rothenberg E, Stein R (1995) Apoptosis induced by serum deprivation of PC12 cells is not preceded by growth arrest and can occur at each phase of the cell cycle. Cancer Res 55 : 1242–1247
20. Lohr F, Wenz F, Haas S, Flentje M (1995) Comparison of proliferating cell nuclear antigen (PCNA) staining and BrdUrd-labelling index under different proliferative conditions in vitro by flow cytometry. Cell Prolif 28 : 93–104
21. Lorico A, Toffoli G, Boicchi M, Erba E, Broggini M, Rappa G, D'Incali M (1988) Accumulation of DNA strand breaks in cells exposed to methotrexate or N^{10}-propargyl-5,8-dideazafolic acid. Cancer Res 48 : 2036–2041
22. Matsui S, Arrendondo M, Toth K, Minderman H, Wrzosek C, Rustum Y (1995) ZD1694-induced cell cycle arrest in human colon carcinoma cell lines expressing wild and mutant p53. Proc Am Assoc Cancer Res 36 : 183A
23. Moran RG (1992) Folate antimetabolites inhibitory to de novo purine synthesis. In: Muggia FM (ed) New drugs, concepts and results in cancer chemotherapy. Kluwer Academic Publishers, Boston, pp 65–87
24. Mosmann T (1983) Rapid colorimetric assay for cellular growth and survival: application to proliferation and cytotoxicity assays. J Immunol Methods 65 : 55–63
25. Pandero A, Yin M, Voigt W, Rustum YM (1995) Contrasting patterns of DNA fragmentation induced by thymidylate synthase inhibitors, ZD1694 and AG331. Oncol Res 7 : 73–81
26. Pizzorno G, Moroson BA, Cashmore AR, Beardsley GP (1991) (6R)-5,10-dideaza-5,6,7,8-tetrahydrofolic acid effects on nucleotide metabolism in CCRF-CEM human T-lymphoblast leukemia cells. Cancer Res 51 : 2291–2295
27. Robinson JP (ed) (1993) Handbook of flow cytometry methods. Wiley, New York Chichester Brisbane Toronto Singapore, p 97
28. Savage JRK, Prasad R (1988) Generalized blocking in S phase by methotrexate. Mutat Res 201 : 195–201
29. Schober C, Gibbs JF, Yin M, Slocum HK, Rustum YM (1994) Cellular heterogeneity in DNA damage and growth inhibition induced by ICI D1694, thymidylate synthase inhibitor, using single cell assays. Biochem Pharmacol 48 : 997–1002
30. Schultz R, Andis S, Chen V, Mendelsohn L, Patel V, Shih C, Houghton J (1996) Comparative antitumor activity of the multitargeted antifolate LY231514 and the thymidylate synthase (TS) inhibitor ZD1694. Proc NCI-EORTC Symp 9 : 290A
31. Shih C, Gossett L, Gates S, MacKellar W. Mendelsohn L, Soose D, Patel V, Kohler W, Ratnam M (1996) LY231514 and its polyglutamates exhibit potent inhibition against both human dihydrofolate reductase (DHFR) and thymidylate synthase (TS): multiple folate enzymes inhibition. Proc NCI-EORTC Symp 9 : 289A
32. Smith GK, Duch DS, Dev IK, Kaufmann SH (1992) Metabolic effects and kill of human T-cell leukemia by 5-deazaacyclotetrahydrofolate, a specific inhibitor of glycineamide ribonucleotide transformylase. Cancer Res 52 : 4895–4903
33. Smith SG, Lehman NL, Moran RG (1993) Cytotoxicity of antifolate inhibitors of thymidylate and purine synthesis to WiDR colonic carcinoma cells. Cancer Res 53 : 5697–5706
34. Sokoloski JA, Pizzorno G, Beardsley GP, Sartorelli AC (1993) Evidence for a relationship between intracellular GTP levels and the induction of HL60 leukemia cell differentiation by 5,10-dideazatetrahydrofolic acid (DDATHF). Oncol Res 5 : 293–299
35. Taylor EC, Kuhnt D, Shih C, Rinzel SM, Grindey GB, Barredo J, Jannatipour M, Moran RG (1992) A dideazatetrahydrofolate analogue lacking a chiral center at C-6,N-[4-[2-(2-amino-3, 4-dihydro-4-oxo-7H-pyrrolo[2, 3-d]pyrimidin-5-yl)ethyl]benzoyl]-L-glutamic acid, is an inhibitor of thymidylate synthase. J Med Chem 35 : 4450–4454
36. Taylor IW, Tattersall MHN (1991) Methotrexate cytotoxicity in cultures of human leukemic cells studied by flow cytometry. Cancer Res 41 : 1549–1558
37. Taylor IW, Slowiaczek P, Francis PR, Tattersall MHN (1982) Purine modulation of methotrexate cytotoxicity in mammalian cell lines. Cancer Res 42 : 5159–5164

38. Taylor IW, Slowiaczek P, Francis PR, Tattersall MHN (1982) Biochemical and cell cycle perturbations in methotrexate-treated cells. Mol Pharmacol 21 : 204–210
39. Tsurusawa M, Niwa M, Katano N, Fujimoto T (1988) Flow cytometric analysis by bromodeoxyuridine/DNA assay of cell cycle perturbation of methotrexate-treated mouse L1210 leukemia cells. Cancer Res 48 : 4288–4293
40. Tsurusawa M, Niwa M, Katano N, Fujimoto T (1990) Methotrexate cytotoxicity as related to irreversible S phase arrest in mouse L1210 leukemia cells. Jpn J Cancer Res 81 : 85–90
41. Vanderplasschen A, Hanon E, Pastoret PP (1995) Flow cytometric measurement of total DNA and incorporated 5-bromo-2′-deoxy-uridine using an enzymatic DNA denaturation procedure. Biochemica 1 : 21
42. Wallen-Ohman M, Lonnbro P, Schon A, Borrebaeck CAK (1993) Antibody-induced apoptosis in a human leukemia cell line is energy dependent: thermochemical analysis of cellular metabolism. Cancer Lett 75 : 103–109
43. Ward WJ, Kimbell R, Jackman AL (1992) Kinetic characteristics of ICI D1694: a quinazoline antifolate which inhibits thymidylate synthase. Biochem Pharmacol 43 : 2029–2031